Clays and Clay Minerals, Vol. 42, No. 5, 561–566, 1994.

^{2}H NMR STUDY OF HYDROGEN BONDING IN DEUTERATED KAOLINITE

SHIGENOBU HAYASHI,[1,2] ETSUO AKIBA,[1] RITSURO MIYAWAKI,[3] AND SHINJI TOMURA[3]

[1] National Institute of Materials and Chemical Research, Tsukuba, Ibaraki 305, Japan

[2] Department of Chemistry, University of Tsukuba, Tsukuba, Ibaraki 305, Japan

[3] National Industrial Research Institute of Nagoya, Kita-ku, Nagoya 462, Japan

Abstract—^{2}H NMR spectra of synthetic deuterated kaolinite have been collected in the temperature range from 150 K to 350 K. Hydroxyl groups show a Pake doublet pattern with an asymmetry factor of 0. They are almost fixed spatially, and undergo a wobbling motion with increasing temperature. The quadrupole coupling constant is 273 ± 3 kHz at 150 K, which indicates that interlayer hydrogen bonding is relatively weak.

Key Words—^{2}H NMR, Kaolinite, Hydrogen bond.

INTRODUCTION

Kaolinite, $Al_2Si_2O_5(OH)_4$, has a dioctahedral 1:1 layer structure consisting of an aluminum hydroxide octahedral sheet and a silica tetrahedral sheet. Many studies have been conducted to clarify the crystal structure. Although the positions of non-hydrogen atoms have been well established, the positions of hydrogen atoms were in controversy until recently (Adams 1983; Young and Hewat 1988; Bish and Deele 1989). Recent neutron powder diffraction studies have concluded space group C1 (Bish 1993; Akiba *et al* 1994).

In the C1 symmetry there are four crystallographically distinct hydrogen atoms; one belongs to an inner hydroxyl group and the other three to inner-surface hydroxyl groups. The latter form interlayer hydrogen bondings. Many compounds can intercalate between kaolinite layers; for example, formamides, acetamides, dimethylsulfoxide (S. Olejnik *et al* 1968, 1970; Costanzo and Giese 1990), fatty acids (Sidheswaren *et al* 1990), alkali acetates (Costanzo and Giese 1990), and alkali halides (Thompson *et al* 1992). Intercalation drastically modifies the nature of the interlayer hydrogen bonding, as has been observed in infrared spectroscopy (S. Olejnik *et al* 1970; Costanzo and Giese 1990; Sidheswaren *et al* 1990; Thompson *et al* 1992). Therefore, study of interlayer hydrogen bonding is considered to be important to understand the intercalation behavior.

Nuclear magnetic resonance (NMR) spectroscopy is suitable to study local structures of short-range order and chemical environments, especially when high-resolution solid-state techniques are used. In previous works, we have measured ^{29}Si and ^{27}Al magic-angle-spinning spectra and ^{1}H wide-line and CRAMPS (Combined Rotation and Multiple Pulse Spectroscopy) spectra (Hayashi *et al* 1992a, 1992b). The presence of two crystallographically distinct sites was confirmed for Si and Al atoms. ^{1}H spectra demonstrated that hydroxyl groups are in a rigid lattice state, i.e., spatially fixed.

^{2}H nucleus has a spin quantum number of 1, and its quadrupole interaction is very sensitive to hydrogen bonding and dynamic properties. In the present work, we have studied environments of hydrogen in kaolinite by measuring ^{2}H NMR spectra of synthetic deuterated kaolinite, and have discussed the nature of hydrogen bonding in kaolinite. To our knowledge, this is the first application of ^{2}H NMR to kaolinite.

EXPERIMENTAL

Tomura *et al* have succeeded in preparation of synthetic kaolinite (Tomura *et al* 1983, 1985). Deuterated kaolinite was synthesized according to the procedure described previously (Miyawaki *et al* 1991), where D_2O was used instead of H_2O (Akiba *et al* 1994). Silica sol and alumina sol (Snowtex-N and Aluminasol-200; Nissan Chemical Industries, Ltd.) were mechanically mixed in a Si:Al ratio of 1:1 and heated at 873 K for 8 h. The mixture was crushed and passed through a 70 mesh sieve. Four grams of the mixture and 16 cm^3 of heavy water (Wako Pure Chemical Industries, Ltd., >99.75%) were placed in a Teflon-coated pressure vessel with a capacity of 25 cm^3 (San-ai Kagaku, Ltd.) and heated at 493 K for 10 days in an electric furnace. The synthesized sample was kept in a dry box filled with argon gas to prevent from the effect of moisture, since replacement of OD groups by OH takes place after prolonged contact with H_2O. Before NMR measurements, the sample was evacuated at 373 K for 0.5 h to remove molecular water adsorbed on the outer surface. Thereafter, it was sealed in a Pyrex ampoule under vacuum.

^{2}H NMR spectra were recorded by a Bruker MSL400 pulsed spectrometer with a static magnetic field strength

Copyright © 1994, The Clay Minerals Society

https://doi.org/10.1346/CCMN.1994.0420507 Published online by Cambridge University Press

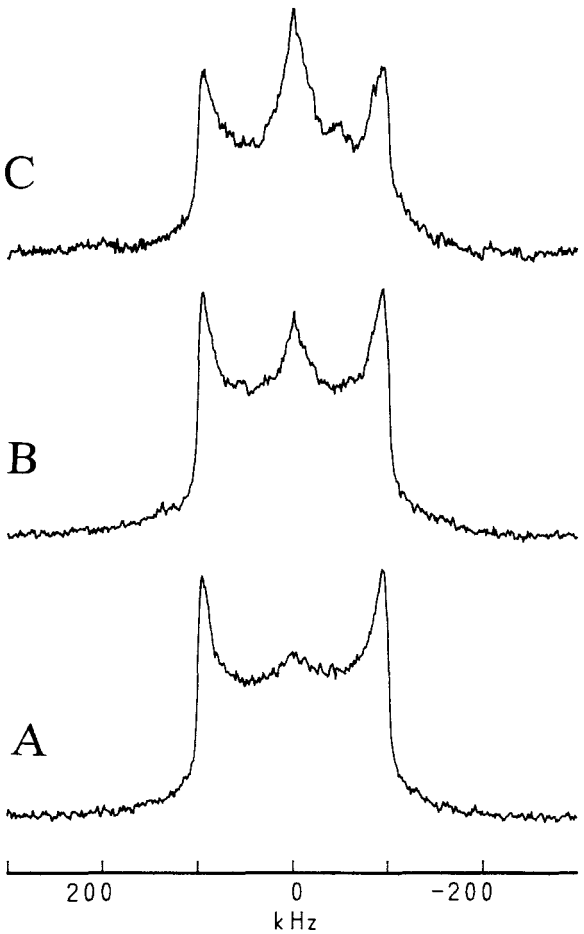

Figure 1. ^2H NMR spectra of deuterated kaolinite, measured at 293 K. The pulse interval τ was set at 15 μs, and the recycle time was varied as follows; (A) 30 s, (B) 0.5 s, and (C) 0.1 s.

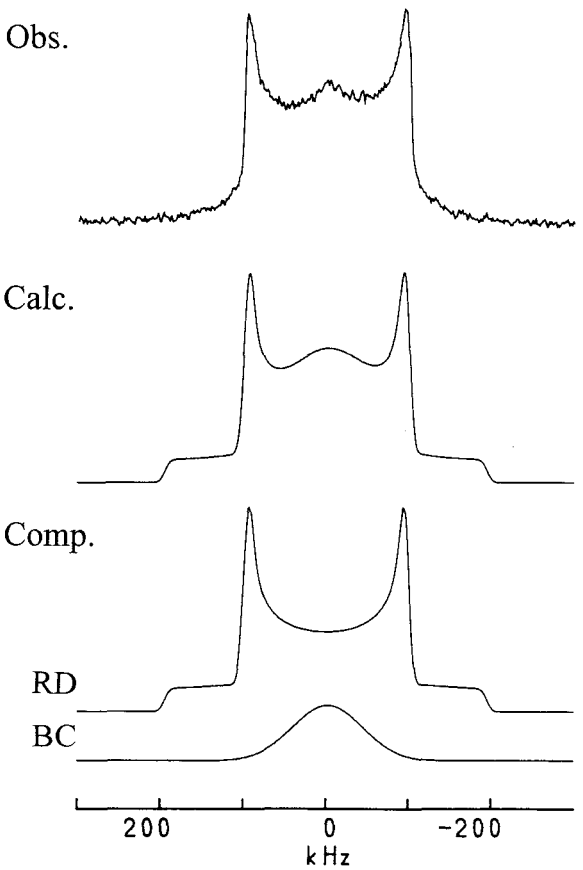

Figure 2. Simulation of a ^2H NMR spectrum shown in Figure 1A.

of 9.4 T. ^2H Larmor frequency was 64.42 MHz. The quadrupole echo pulse sequence, $90°_x$ pulse—delay τ—$90°_y$ pulse—delay τ—echo signal—recycle delay, was used, and the latter half of the echo signal was Fourier-transformed to obtain spectra. The 90° pulse width was 3.7 μs, while the delay τ was varied. The sample was static, and its temperature was varied between 150 K and 350 K by means of N_2 gas flow which was temperature-controlled. The frequency scale of the spectra was expressed with respect to D_2O. The line shapes of the spectra were analyzed using our computer programs (Hayashi *et al* 1991).

^1H NMR spectra were also measured by the Bruker MSL400 spectrometer in order to check the amount of O-H groups, which was less than 2% of the ideal hydrogen content for non-deuterated kaolinite.

The same sample was subjected to X-ray powder diffraction, infrared spectroscopy, and thermogravimetric analysis, whose results were published elsewhere (Miyawaki 1994; Akiba *et al* 1994). The X-ray diffraction pattern of the deuterated sample was identical with that of a non-deuterated synthetic sample, and Hinckley index was 0.8. O-D stretching bands were observed in the region 2750–2650 cm^{-1} of infrared spectra in place of O-H bands (3700–3600 cm^{-1}). Kaolinite content was evaluated from a weight loss upon heating, which was about 90 wt. %. The sample was considered to contain 10 wt. % of amorphous materials, since no extra peaks were observed in the X-ray diffraction pattern.

RESULTS AND DISCUSSION

Figure 1 shows ^2H NMR spectra measured at 293 K for a static sample. The intensity of the central portion increases as the recycle time becomes longer, indicating the presence of different species. Therefore, the spectra are deconvoluted into two components, a resolved doublet (RD) and a broad central (BC), as shown in Figure 2. The BC component is assumed to have a Gaussian-like line shape. The relative intensity of the BC component increases with decreasing recycle time (see Figures 1A, 1B and 1C). Since decreasing recycle time favors the collection of components with short spin-lattice relaxation times, the BC component has a shorter relaxation time than the RD component

https://doi.org/10.1346/CCMN.1994.0420507 Published online by Cambridge University Press

does. Since the BC component recovers within the recycle time of 0.1 s, the spin-lattice relaxation time is much shorter than 0.1 s. The amount is about 2% of the total deuterium content in fully deuterated kaolinite. This component is ascribed to O-D groups in amorphous regions, where the O-D groups are mobile, causing rapid relaxation of the magnetization. The BC component is neglected in the discussion below.

The RD component is ascribed to kaolinite O-D groups, which appear to be in an almost rigid state from the simulated pattern shown in Figure 2, called Pake doublet pattern. The quadrupole coupling constant (e^2Qq/h) and the asymmetry factor (η) used for the simulation are 260 kHz and 0.0, respectively.

The spin-lattice relaxation time of the RD component was measured by the inversion recovery method. The relaxation curve shows a slight nonexponentiality initially, and it decays exponentially at a sufficiently long time. This behavior indicates that the relaxation is caused by paramagnetic impurities and that spin diffusion between ^{2}H spins limits the relaxation rate. The spin-lattice relaxation time in the diffusion-limited region is 5.3 s. Consequently, Figure 1A shows a spectrum in a fully relaxed state, whereas the intensity of the RD component is suppressed in Figures 1B and 1C. O-D motions can relax the ^{2}H magnetization efficiently, if they exist. The relatively long relaxation time demonstrates no contribution of the motion.

The line shape of ^{2}H NMR spectra is also sensitive to hydrogen motion. Although the resolved doublet line shape indicates a rigid nature of this component already, we investigate the motion in more detail. First, the line shape should depend on the interval between the two pulses in the quadrupole echo sequence if a motion takes place at a frequency corresponding to the pulse interval. No clear dependence was obtained at 293 K when the interval τ was varied from 15 μs to 800 μs. Thus, a motion with a time constant of the order of 100 μs is absent.

Next, we have measured temperature dependence of ^{2}H NMR spectra, as shown in Figure 3. The Pake doublet pattern is observed over the temperature range studied, indicating that no motions with large amplitudes initiate in this temperature range. However, the line shape changes slightly with temperature. Quadrupole interaction parameters extracted from the simulation are listed in Table 1, and quadrupole coupling constants are plotted as a function of temperature in Figure 4. At the lowest temperature (150 K), the RD component has a quadrupole coupling constant of 273 kHz and an asymmetry factor of 0. The residual linewidth after subtracting the contributions from the dipole-dipole interaction and from smoothing in the Fourier transformation process is regarded as coming from the distribution of the coupling constant. A linewidth originated from the dipole-dipole interaction between ^{2}H spins and between a ^{2}H spin and ^{27}Al spins

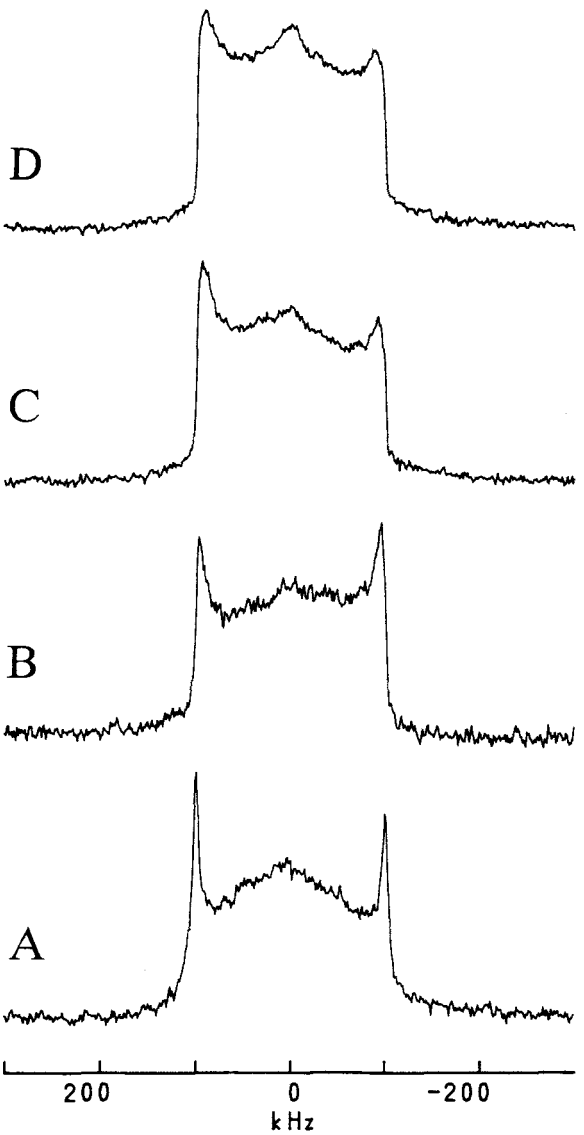

Figure 3. Temperature dependence of ^{2}H NMR spectra of deuterated kaolinite. The pulse interval and the recycle time were set at 15 μs and 50 s, respectively. The sample temperatures were (A) 150 K, (B) 250 K, (C) 305 K, and (D) 350 K.

is 1.9 kHz, being estimated from the crystal structure. The line broadening in the Fourier transformation process was set at 1.0 kHz. At 150 K, distribution of the quadrupole coupling constant is ± 3 kHz, where a Gaussian distribution function is assumed. The width of the distribution increases with temperature. The line shape cannot be simulated by one RD component at and above 305 K, even if η is adjusted. This means that the distribution is too wide to be described by one Gaussian function. Figure 5B shows a calculated spectrum using one RD component with $\eta \neq 0$, but the experimental line shape cannot be reproduced. Therefore, we have assumed the presence of two RD com-

https://doi.org/10.1346/CCMN.1994.0420507 Published online by Cambridge University Press

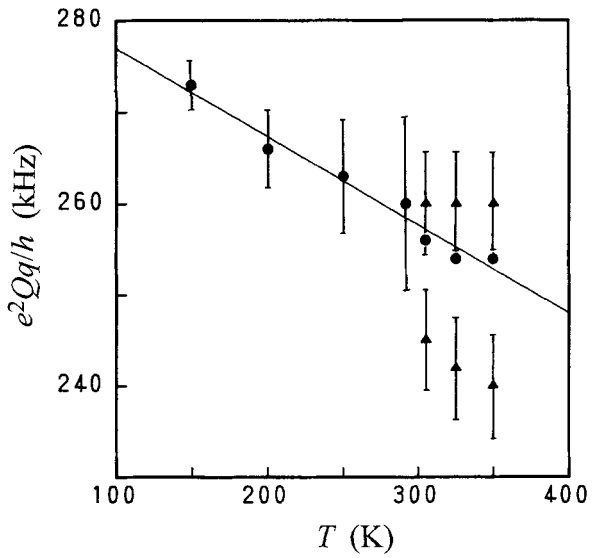

Figure 4. Temperature dependence of the quadrupole coupling constant for the RD component. The solid circles indicate the average values. The solid triangles at and above 305 K show the values of each component used in the simulation. Bars on the symbols indicate the distribution of the coupling constant, assuming a Gaussian distribution function. The straight line is drawn with a least square fit.

ponents, which means that the distribution of the coupling constant is assumed to be described by two Gaussian functions. The calculated spectra of the two-RD-component analysis are shown in Figure 5A, and the obtained parameters are listed in Table 1. The obtained asymmetry factor is always 0. The weighted average value of the quadrupole coupling constant, shown by solid circles in Figure 4, decreases linearly with temperature, being expressed as

$$e^2Qq/h = 286.7 - 0.10\ T, \qquad (1)$$

where e^2Qq/h and T are in units of kHz and K, respectively.

The temperature dependence of the quadrupole coupling parameters described above is considered to originate from motions of O-D groups, although the amplitude of the motions should be small. The average value of the quadrupole coupling constant decreases with temperature, keeping $\eta = 0$. If the O-D group rotates around an axis which is inclined at an angle θ, as illustrated in Figure 6, the effective asymmetry factor remains zero while the effective quadrupole coupling constant is reduced by a factor of $(3\cos^2\theta - 1)/2$ (Barnes 1974). Rotations around a more than two-fold axis also show similar spectral features. The most likely motion

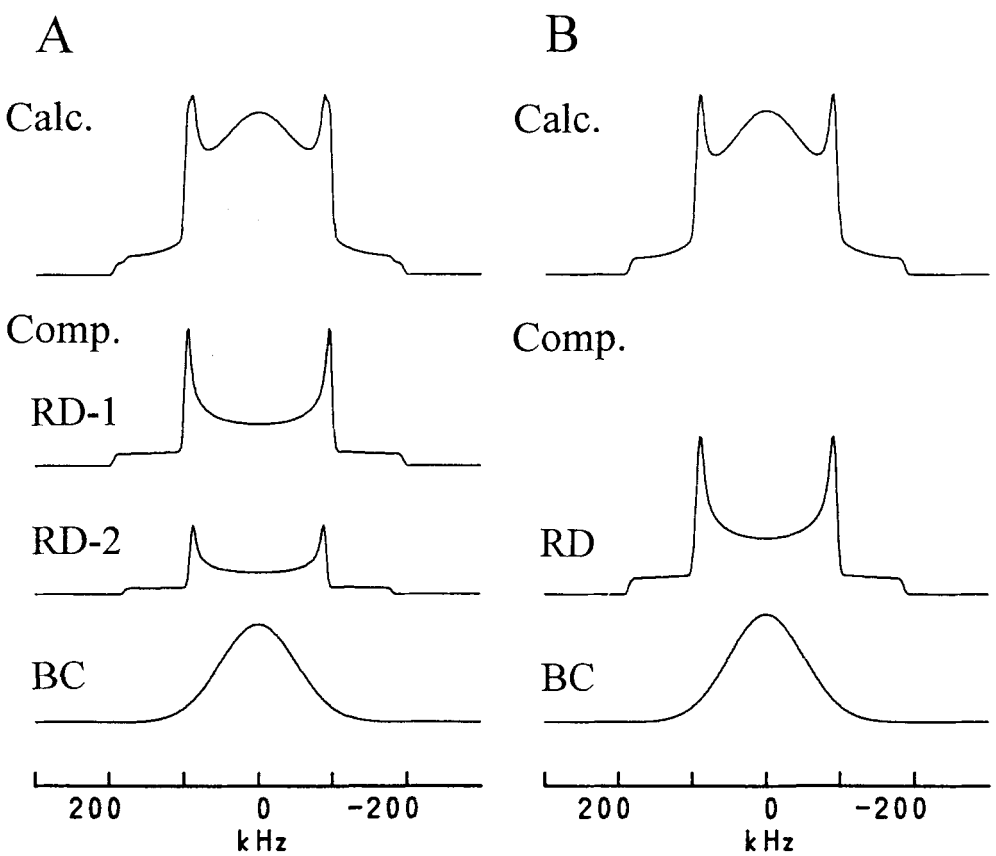

Figure 5. Simulation of a ^2H NMR spectrum shown in Figure 3D. Calculated spectra were obtained, assuming presences of (A) two RD components with $\eta = 0$ and (B) one RD component with $\eta = 0.03$ other than one BC component.

https://doi.org/10.1346/CCMN.1994.0420507 Published online by Cambridge University Press

Table 1. Quadrupole interaction parameters for the RD component.

	RD-1			RD-2		
T (K)	e^2Qq/h[1] (kHz)	η	f[2] (%)	e^2Qq/h[1] (kHz)	η	f[2] (%)
150	273 ± 3	0	100			
200	266 ± 4	0	100			
250	263 ± 6	0	100			
293	260 ± 9	0	100			
305	260 ± 5	0	76	245 ± 5	0	24
325	260 ± 5	0	68	242 ± 5	0	32
350	260 ± 5	0	68	240 ± 5	0	32

[1] The value after the symbol ± expresses a width of Gaussian distribution.
[2] Fraction of this component.

is a wobbling motion, where D moves randomly on the bottom surface of the cone shown in Figure 6. The motion should be much faster than the quadrupole coupling constant. The magnitude of θ increases with temperature. If the quadrupole coupling constant extrapolated to 0 K (286.7 kHz) corresponds to the value in the rigid state, the average coupling constant at 350 K (254 MHz) leads to $\theta = 16°$.

The quadrupole coupling constant is related to the strength of hydrogen bonding. In a O-H–O hydrogen bond whose geometry is within 30° of linearity, the coupling constant is expressed empirically as follows;

$$e^2Qq/h = -5414.7 + 4113.7R_{O\text{-}O} - 857.02R_{O\text{-}O}^2 + 38.146R_{O\text{-}O}^3, \quad (2)$$

where $R_{O\text{-}O}$ is a distance between two O atoms in unit of A (Butler and Brown 1981). Eq. (2) was obtained from experimental data for many inorganic hydrate compounds covering $R_{O\text{-}O}$ values between 2.4 and 3.0 A, and the coupling constant is at most 240 kHz for $R_{O\text{-}O}$ = 3.0 A. The coupling constant of deuterated kaolinite is larger than the above range and indicates that the hydrogen bond is relatively weak. The average $R_{O\text{-}O}$ value in kaolinite is concluded to be at least 3.0 A.

In our previous work, we have obtained accurate ^{1}H chemical shift values of kaolinite, which was 2.8 ppm from tetramethylsilane with a distribution of ±0.8 ppm (Hayashi *et al* 1992a). Yesinowski *et al* (1987) have proposed an empirical correlation between the ^{1}H chemical shift and the O–O interatomic distances in hydrogen bonding. The chemical shift 2.8 ± 0.8 ppm leads to $R_{O\text{-}O}$ = 2.99 ± 0.03 A, which is consistent with the ^{2}H NMR results.

The coupling constant correlates also with the D–O distance in a O-D–O hydrogen bond ($R_{D\text{-}O}$) (Soda and Chiba 1969), which can be expressed as

$$e^2Qq/h = 310.0 - 3.0 \times 190.6/R_{D\text{-}O}^3, \quad (3)$$

where e^2Qq/h and $R_{D\text{-}O}$ are in units of kHz and A, respectively. The observed e^2Qq/h values, 273 ± 3 kHz (150 K) and 260 ± 9 kHz (293 K) lead to $R_{D\text{-}O}$ values

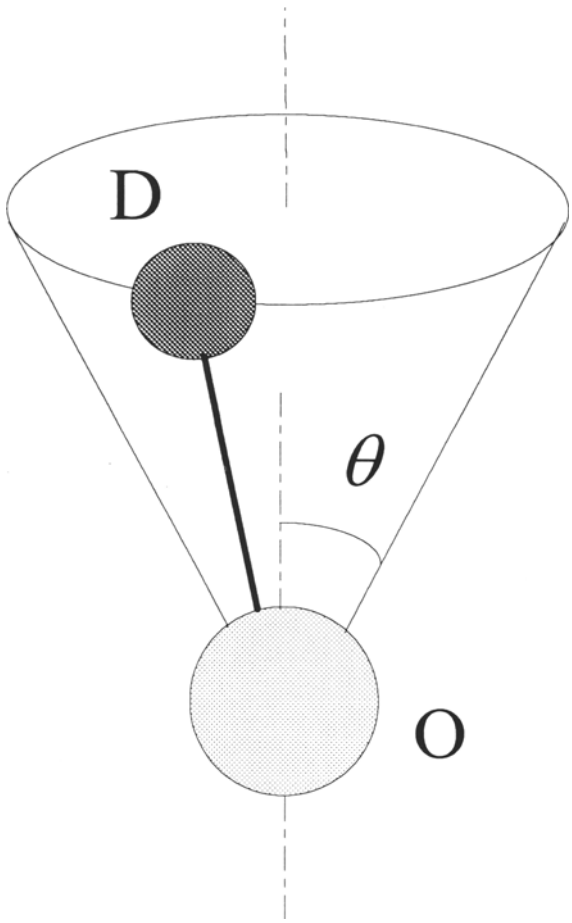

Figure 6. A model of the O-D motion.

of 2.49 ± 0.07 A and 2.25 ± 0.16 A, respectively. Those values should be considered to be roughly estimated values, since the above empirical correlation contains a considerable magnitude of data dispersion.

There are four crystallographically inequivalent sites for hydrogen atoms. The present ^{2}H NMR results cannot separate the environments of the four hydrogen sites. The quadrupole coupling constant reflects a electric field gradient at the nucleus site made by surrounding electrons. The electronic environments of the four O-D groups are very much similar to each other. With increasing temperature the dispersion of the quadrupole coupling constant increases and finally the distribution is described by two Gaussians. One O-D group among the four might have a slightly different dynamic property.

The crystal structure has recently been refined by Bish (1993). The $R_{O\text{-}O}$ values in the interlayer hydrogen bondings are 2.945, 2.980 and 3.087 A, which were related to infrared absorption bands at 3651, 3668 and 3696 cm^{-1}, respectively. The shorter $R_{O\text{-}O}$ corresponds to the lower frequency infrared band, having the stron-

https://doi.org/10.1346/CCMN.1994.0420507 Published online by Cambridge University Press

ger hydrogen bonding. The inner hydroxyl group has an infrared band at about 3620 cm^{-1}, which is shifted to lower frequency, although the hydrogen bonding is weaker than the others. The R_{O-O} values roughly estimated from the ^2H results are consistent with the crystal structure.

The refinement of the crystal structure also presented the presence of anisotropic positional disorders at 1.5 K (Bish 1993). The hydrogens in inner hydroxyls exhibit the largest amount of positional disorder perpendicular to the layers, whereas those of the inner-surface hydroxyl groups exhibits the largest amount of positional disorder within the plane of layers. These positional disorder might develop into thermal motions as modeled in Figure 6 with increasing temperature.

In summary, we have measured ^2H NMR spectra of synthetic deuterated kaolinite in the temperature range from 150 K to 350 K. The spectra consist of two components; a resolved doublet component ascribed to hydroxyl groups in kaolinite and a broad central component coming from mobile hydroxyl groups in amorphous regions. ^2H NMR cannot separate the environments of the four crystallographically inequivalent hydrogen sites, and the electronic environments of the four O–D groups are very much similar to each other. The large quadrupole coupling constant indicates that interlayer hydrogen bonding is relatively weak. The hydroxyl groups undergo a wobbling motion of small amplitudes with increasing temperature.

REFERENCES

Adams, J. M. 1983. Hydrogen atom positions in kaolinite by neutron profile refinement. *Clays & Clay Miner.* **31**: 352–356.

Akiba, E., H. Hayakawa, H. Asano, F. Izumi, R. Miyawaki, S. Tomura, and Y. Shibasaki. 1994. Structure refinement of artificial deuterated kaolinite by Rietveld analysis using Time-of-Flight neutron powder diffraction data. *Clays & Clay Miner.*: submitted.

Barnes, R. G. 1974. Deuteron quadrupole coupling tensors in solids. *Adv. Nucl. Quadrupole Reson.* **1**: 335–355.

Bish, D. L. 1993. Rietveld refinement of the kaolinite structure at 1.5 K. *Clays & Clay Miner.* **41**: 738–744.

Bish, D. L., and R. B. Von Dreele. 1989. Rietveld refinement of non-hydrogen atomic positions in kaolinite. *Clays & Clay Miner.* **37**: 289–296.

Butler, L. G., and T. L. Brown. 1981. Nuclear quadrupole coupling constants and hydrogen bonding. A molecular orbital study of oxygen-17 and deuterium field gradients in formaldehyde-water hydrogen bonding. *J. Am. Chem. Soc.* **103**: 6541–6549.

Costanzo, P. M., and R. F. Giese, Jr. 1990. Ordered and disordered organic intercalates of 8.4-A, synthetically hydrated kaolinite. *Clays & Clay Miner.* **38**: 160–170.

Hayashi, S., K. Hayamizu, S. Mashima, A. Suzuki, P. J. McElheny, S. Yamasaki, and A. Matsuda. 1991. ^2D and ^1H nuclear magnetic resonance study of deuterated amorphous silicon and partially deuterated hydrogenated amorphous silicon. *Jpn. J. Appl. Phys.* **30A**: 1909–1914.

Hayashi, S., T. Ueda, K. Hayamizu, and E. Akiba. 1992a. NMR study of kaolinite. 1. ^{29}Si, ^{27}Al, and ^1H spectra. *J. Phys. Chem.* **96**: 10922–10928.

Hayashi, S., T. Ueda, K. Hayamizu, and E. Akiba. 1992b. NMR study of kaolinite. 2. ^1H, ^{27}Al, and ^{29}Si spin-lattice relaxations. *J. Phys. Chem.* **96**: 10928–10933.

Miyawaki, R. 1994. Hydrothermal synthesis of kaolinite. *J. Clay Sci. Soc. Japan* **33**: 202–214.

Miyawaki, R., S. Tomura, S. Samejima, M. Okazaki, H. Mizuta, S. Maruyama, and Y. Shibasaki. 1991. Effects of solution chemistry on the hydrothermal synthesis of kaolinite. *Clays & Clay Miner.* **39**: 498–508.

Olejnik, S., L. A. G. Aylmore, A. M. Posner, and J. P. Quirk. 1968. Infrared spectra of kaolin mineral-dimethyl sulfoxide complexes. *J. Phys. Chem.* **72**: 241–249.

Olejnik, S., A. M. Posner, and J. P. Quirk. 1970. The intercalation of polar organic compounds into kaolinite. *Clay Miner.* **8**: 421–434.

Sidheswaren, P., A. N. Bhat, and P. Ganguli. 1990. Intercalation of salts of fatty acids into kaolinite. *Clays & Clay Miner.* **38**: 29–32.

Soda, G., and T. Chiba. 1969. Deuteron magnetic resonance study of cupric sulfate pentahydrate. *J. Chem. Phys.* **50**: 439–455.

Thompson, J. G., P. J. R. Uwins, A. K. Whittaker, and I. D. R. Mackinnon. 1992. Structural characterization of kaolinite : NaCl intercalate and its derivatives. *Clays & Clay Miner.* **40**: 369–380.

Tomura, S., Y. Shibasaki, H. Mizuta, and M. Kitamura. 1983. Spherical kaolinite: Synthesis and mineralogical properties. *Clays & Clay Miner.* **31**: 413–421.

Tomura, S., Y. Shibasaki, H. Mizuta, and M. Kitamura. 1985. Growth conditions and genesis of spherical and Platy kaolinite. *Clays & Clay Miner.* **33**: 200–206.

Yesinowski, J. P., and H. Eckert. 1987. Hydrogen environments in calsium phosphates. *J. Am. Chem. Soc.* **109**: 6274–6282.

Young, R. A., and A. W. Hewat. 1988. Verification of the triclinic crystal structure of kaolinite. *Clays & Clay Miner.* **36**: 225–232.

(Received 10 April 1993; accepted 10 May 1994; Ms. 2427)

https://doi.org/10.1346/CCMN.1994.0420507 Published online by Cambridge University Press